RSC Advances

PAPER

View Article Online
View Journal | View Issue

Cite this: *RSC Adv.*, 2017, **7**, 31641

Synthesis and application of polyzwitterionic and polyampholytic maleic acid-*alt*-(diallylamino) propylphosphonates

Ibrahim Y. Yaagoob, Hasan A. Al-Muallem * and Shaikh A. Ali*

Ammonium persulfate-initiated alternate copolymerization of maleic acid with phosphonic acid monomer $[(CH_2{=}CH{-}CH_2)_2NH^+(CH_2)_3PO_3H_2Cl^-]$ (**I**) and phosphonate ester monomer $[(CH_2{=}CH{-}CH_2)_2NH^+(CH_2)_3PO_3Et_2Cl^-]$ (**II**) gave polyzwitterion (PZ): poly[(**I**–HCl)-*alt*-maleic acid] **III** and polyampholyte (PA): poly[(**II**)-*alt*-maleic acid] **IV**, respectively. PA **IV**, upon ester hydrolysis, gave PZ **III**. The pH-induced changes of backbone charges in tetraprotic **III** (with respect to each repeating unit) and diprotic **IV** were examined by viscosity measurements. PA **IV** exhibited antipolyelectrolyte character in the presence of neutral salt NaCl. Several protonation constants *K* of the CO_2^- and trivalent nitrogen in **III** and **IV** have been determined. The performance evaluation as a potential antiscalant in reverse osmosis (RO) plants was examined. **III** containing acid motifs of $-PO_3H_2$ at a concentration of 15 ppm demonstrated remarkable efficiency of ≈100% in inhibition of $CaSO_4$ scale from its supersaturated solution for several days at 40 °C, while precipitation occurred within 10 min in the presence of 20 ppm of **IV** containing ester motifs of $-PO_3Et_2$.

Received 19th April 2017
Accepted 13th June 2017

DOI: 10.1039/c7ra04418f

rsc.li/rsc-advances

1. Introduction

Butler's cyclopolymerization protocol[1,2] using diallylammonium salt monomers has etched an important place in the synthesis of a variety of ionic polymers of remarkable industrial significance.[3–5] This industrially important protocol is known to lead to the formation of a pyrrolidine ring-embedded backbone considered to be the eighth most important architecture for high polymers.[2,6] Butler's cyclopolymer poly(diallyldimethylammonium chloride) has numerous publications and patents (>1000);[1] millions of pounds of poly(diallyldimethylammonium chloride) are sold annually for water treatment.[1] The polymers from diallylamine salts $[(CH_2{=}CH{-}CH_2)_2NH^+RCl^-]$, bearing pH-responsive backbone nitrogens and functionalities in the pendants (R), undergo pH-induced transformation to polymers having charges of both algebraic signs in the chains.[5,7,8] The bio-mimicking polyampholytes (+ −)[9,10] and polyzwitterions (±)[11] have found applications in the field of biotechnology, medicine, oil industry, hydrometallurgy and desalination.[12]

The effectiveness of a desalination process depends on the mitigation of scale formation leading to membrane fouling. In reverse osmosis (RO) membrane desalination, as the concentration of salts, such as calcium sulfate, calcium carbonate, barium sulfate and strontium sulfate, *etc.*, exceeds their saturation levels, the crystallization (*i.e.* scale formation) on membrane surfaces results in the decline of permeate flux. The feed passages are also often plugged by the scale. There are three commonly employed methods of scale control: acidification, ion exchange softening and antiscalant addition. Antiscalants are surface active materials that interfere with precipitation reactions to keep the scaling salts in supersaturated state.[13] As a crystal begins to grow, an antiscalant is adsorbed on its surface thereby disrupting the crystal growth and leading to a soft non-adherent distorted scale. An antiscalant can act as a dispersant; upon adsorption onto a crystal surface, it imparts high anionic charges to keep the crystals separated. The active ingredients in commercial antiscalants are mostly proprietary mixtures of various polycarboxylates and polyacrylates, condensed polyphosphates and organophosphonates.[13–15]

In this paper, with judicious choice of monomers, Butler cyclopolymerization protocol is utilized to decorate the repeating units with both the carboxylate and phosphonate motifs which are potent functionalities to impart antiscalant behavior. Thus, we report for the first time the copolymerization of **1**, **11** and **12** (containing phosphonate pendants) with maleic acid (**2**) to pH-responsive alternate copolymers (Schemes 1 and 2). The study would examine the mechanism of alternation, the pH-induced transformation and the efficacy of the copolymers as antiscalants.

2. Experimental

2.1. Materials

Ammonium persulfate (APS), 2,2′-azobis(2-methylpropionamidine) dihydrochloride (AMPH) from Sigma-Aldrich, and maleic acid from BDH Chemicals Ltd., Poole, England,

Chemistry Department, King Fahd University of Petroleum & Minerals, Dhahran 31261, Saudi Arabia. E-mail: hmuallem@kfupm.edu.sa; shaikh@kfupm.edu.sa; Web: http://www.faculty.kfupm.edu.sa/CHEM/hmuallem/; Fax: +966 13 860 4277; Tel: +966 13 860 2378

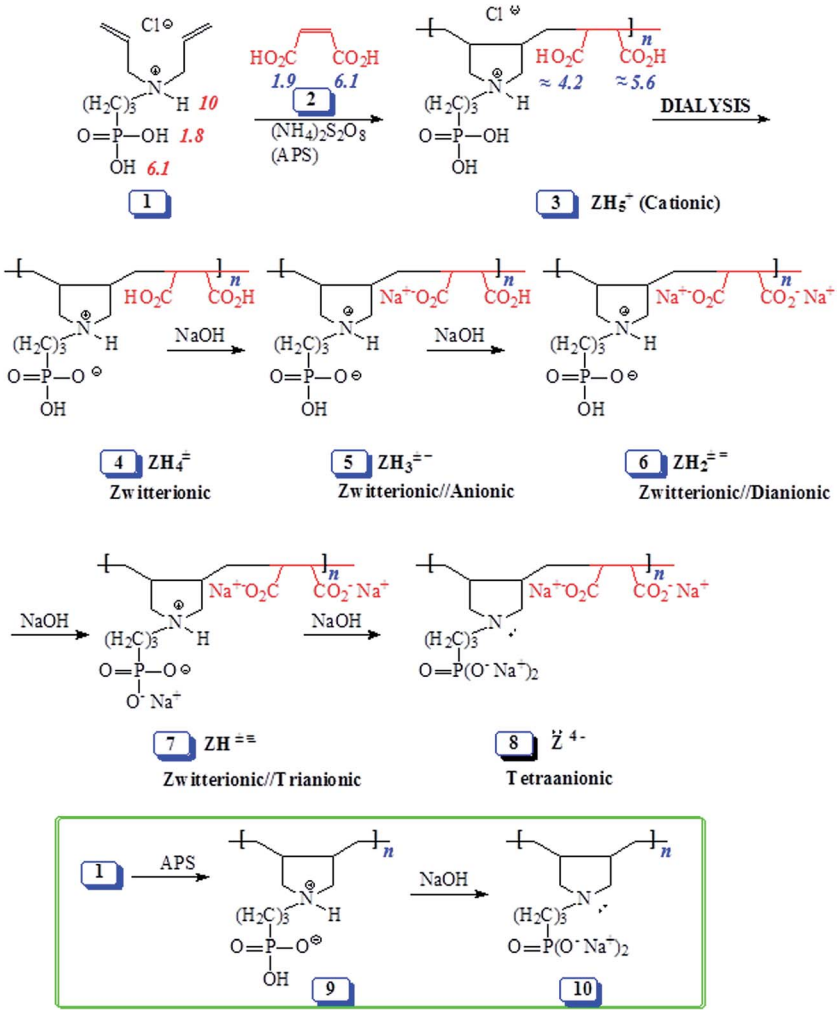

Scheme 1 Synthesis of alternate copolymers from monomer **1**/maleic acid **2** using cyclopolymerization protocol.

were used as received. Trivalent amine **11** and its hydrochloride salt **12** were prepared as described.[16,17] 3-(*N*,*N*-Diallylamino)propanephosphonic acid (**1**) was obtained by means of hydrolysis of **11** following the reported procedure.[18] The molar mass of **1** was determined to be 277 g mol^{-1} using ^{1}H NMR integration of several non-overlapping signals of the monomer and a known concentration of ethanol. It is difficult to remove the strenuous HCl present in the sample. Note that the calculated molar mass of **1** is 255.68 g mol^{-1}. As such, in subsequent polymerization, the monomer is considered to have a purity of 92%. Spectra/Por membrane with MWCO of 6000–8000 purchased from Spectrum Laboratories Inc. was used for dialysis.

2.2. Physical methods

A Perkin Elmer Elemental Analyzer Series 11 Model 2400 (Waltham, Massachusetts, USA) was employed to determine elemental composition. A Thermo scientific FTIR spectrometer (Nicolet 6700, Thermo Electron Corporation, Madison, WI, USA) was used to record IR spectra. ^{31}P, ^{1}H and ^{13}C NMR spectra of the polymers were measured in D_2O on a JEOL LA 500 MHz spectrometer. ^{31}P was referenced with 85% H_3PO_4 in DMSO. The residual HOD signal of D_2O at δ 4.65 ppm, and dioxane ^{13}C resonance at δ 67.4 were used as internal references. However, the position of residual proton resonance of D_2O depends on the solution pH; in such cases the chemical shifts were referenced with sodium 3-trimethylsilylpropionate-2,2,3,3-d_4 (TSP-deuterated) having ^{1}H signal at δ 0 ppm. An Ubbelohde viscometer (Viscometer Constant = 0.005718 cSt s^{-1}) was utilized for viscosity measurements. An SDT analyzer (Q600: TA instruments, USA) was utilized for thermogravimetric analyses (TGA) in the range 20–800 °C increasing at rate of 15 °C min^{-1} using N_2 flowing at a rate of 50 cm^3 min^{-1}.

2.3. Polymer synthesis

2.3.1. Copolymerization of 3-(*N*,*N*-diallylamino)propanephosphonic acid (1) and maleic acid (2). The alternate polymerizations were performed under the conditions described in Table 1. In one such case (entry 2, Table 1), APS was added at 98 °C in two equal portions (2 × 200 mg) with an interval of 5 min to a stirred mixture comprised of monomer **1** (2.77 g, 10 mmol) and maleic acid (**2**) (1.28 g, 11 mmol) in water (1.74 g; monomers/water wt ratio is 70 : 30) in a RB flask fitted with

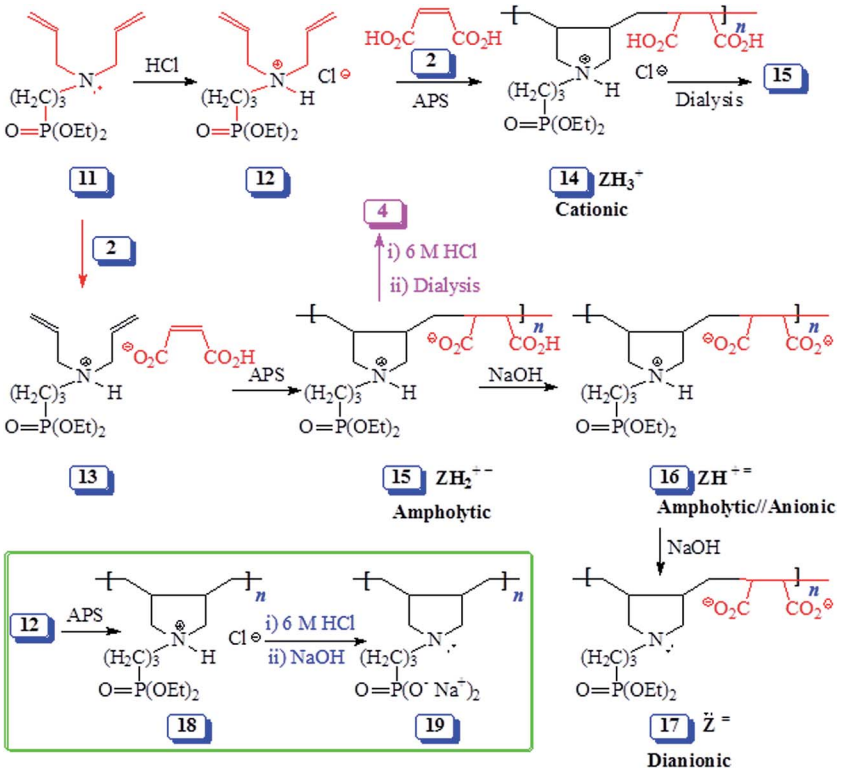

Scheme 2 Synthesis of alternate copolymers from monomer **12**/maleic acid **2** and monomer complex **13** using cyclopolymerization protocol.

a condenser under N_2. After 20 min at 98 °C, the polymer solution was cooled and dialyzed against deionized water. Note that initial polymer **3** became cloudy when diluted with H_2O and clear in dilute HCl. During dialysis against distilled water, a thick cloudy jelly material settled at the bottom of the dialysis tube within an hour. At this stage, dialysis was continued against a 0.3 M HCl which rendered the polymer mixture clear and ensured the removal unreacted maleic acid. On further dialysis against distilled water, the mixture became cloudy and a gel settled at the bottom of the dialysis tube. Afterward (48 h), both the supernatant and the jelly material were subjected to freeze drying to give copolymer **4** (2.5 g, 75%) (found: C 46.2; H 6.8; N 4.1%. $C_{13}H_{22}NO_7P$ requires C 46.57; H 6.61; N 4.18%); δ_P (200 MHz, 2 M NaCl in D_2O): 23.08 (m, 1P); δ_P (200 MHz, in D_2O in the presence of 4 equiv. NaOH): 20.33 (major, 98%, s, 1P), 26.23 (m, minor, 2%); ν_{max} (KBr): 3566 (broad), 2958, 2925, 1717, 1458, 1233, 1122, 1029, 906, 704, 669, 537, and 474 cm^{-1}.

2.3.2. Copolymerization of *N,N*-diallyl-3-(diethylphosphonato)propylamine (11) and maleic acid (2) through ion pair 13. For the experiment under entry 6, Table 1, a mixture of trivalent amine **11** (2.76 g, 10.0 mmol), and maleic acid **2** (1.28 g, 11.0 mmol) in water (1.74 g; monomers/water wt ratio is 70 : 30) was stirred at 98 °C under a positive atmosphere of N_2 in a RB flask attached to a condenser. Then, initiator (APS) was added in two equal portions (2 × 200 mg) with an interval of 5 min. Exothermic polymerization ensued with the increase in viscosity. After stirring at 98 °C (15 min), the mixture was dialyzed against deionized water for 24 h. The dialyzed mixture was then freeze-dried affording alternating copolymer, polyampholyte **15** as a white powder (2.85 g, 73%). δ_P (200 MHz, D_2O): 23.60 (s, minor 10%, 1P), 31.19 (s, major 90%); found: C 51.8; H 7.9; N 3.4%. $C_{17}H_{30}NO_7P$ requires C 52.17; H 7.73; N 3.58. ν_{max} (KBr): 3455 (broad), 2984, 2941, 1712 (s), 1640 (s), 1575 (s), 1451, 1395, 1214, 1051, 1023, 968 and 790 cm^{-1}.

Table 1 Cyclocopolymerization[a] of monomers **1**, **11** and **12** with maleic acid **2**

Entry	Monomer (mmol) **1**	**11**	**12**	**2**	Initiator (APS) (mg)	Yield[b] (%)	$[\eta]^c$ (dL g^{-1})
1	5.0	—	—	5.5	400	**4**: 55 (90)	0.0614[d]
2	5.0	—	—	5.0	300	**4**: 75 (85)	0.0872[d]
3	5.0	—	—	5.5	300	**4**: 72 (93)	0.0581[d]
4	5.0	—	—	11.0	300	**4**: 66 (91)	0.0611[d]
5	—		5.0	5.5	300	**14**: 66 (98)	0.0178
6	—	10.0	—	11.0	400	**15**: 73 (90)	0.0618
7[e]	—	5.0	—	5.5	300	**15**: 82 (94)	0.0253
8[f]	—	5.0	—	5.5	60 (AMPH)	**15**: 45 (60)	0.0657

[a] Copolymerization reactions were carried out in aqueous solution of two monomers (70 w/w% monomers) in the presence of ammonium persulfate (APS) or (AMPH) at 98° C for 20 min. [b] Polymer obtained is written in bold followed by isolated yields; the percent conversion determined by ^1H NMR analyses of the crude reaction mixture are written in parentheses. [c] Viscosity of 1–0.25% polymer solution in 0.1 N NaCl at 30° C was measured with Ubbelohde viscometer (K = 0.005317 mm^2 s^{-2}). [d] In the presence of 1 equiv. NaOH. [e] Polymerization carried out in the presence of 5.0 mmol NaCl. [f] Polymerization was run for 48 h at 80 °C.

Table 2 Protonation of polymer **15** ($ZH_2^{\pm}$) at 23 °C

Run	$ZH_2^{\pm}$ (mmol)	C_T[a] (mol dm^{-3})	α-Range	pH-range	Points[b]	Log K_1^{oc}	n_1[c]	R^{2d}
1	0.2554 ($ZH_2^{\pm}$)	+0.1222	0.03–0.21	3.09–2.75	11	2.54	0.36	0.9916
2	0.2812 ($ZH_2^{\pm}$)	+0.1222	0.05–0.21	3.08–2.81	12	2.57	0.42	0.9887
3	0.3193 ($ZH_2^{\pm}$)	+0.1222	0.06–0.18	3.09–2.85	07	2.59	0.40	0.9934
Average						2.58 (3)	0.41 (4)	
Log $K_3^e = 2.58 - 0.59 \log[(1-\alpha)/\alpha]$ for the reaction: $ZH_2^{\pm} + H^+ \overset{K_1}{\rightleftharpoons} ZH_3^+$								
1	0.2554 ($ZH_2^{\pm}$)	−0.09594	0.87–0.14	3.74–7.74	17	5.82	2.43	0.9989
2	0.3193 ($ZH_2^{\pm}$)	−0.09594	0.88–0.10	4.01–8.10	19	5.83	2.33	0.9964
3	0.3831 ($ZH_2^{\pm}$)	−0.09594	0.85–0.20	4.06–7.20	17	5.74	2.37	0.9965
Average						5.80 (5)	2.38 (5)	
Log $K_2^e = 5.80 + 1.38 \log[(1-\alpha)/\alpha]$ for the reaction: $ZH^{\pm -} + H^+ \overset{K_2}{\rightleftharpoons} ZH_2^{\pm}$								
1	0.2554 ($ZH_2^{\pm}$)	−0.09594	0.91–0.58	9.65–11.06	17	11.29	1.71	0.9911
2	0.3193 ($ZH_2^{\pm}$)	−0.09594	0.90–0.56	9.78–11.17	17	11.36	1.68	0.9964
3	0.3831 ($ZH_2^{\pm}$)	−0.09594	0.88–0.59	9.83–11.04	18	11.31	1.73	0.9967
Average						11.31 (4)	1.71 (3)	
Log $K_1^e = 11.31 + 0.71 \log[(1-\alpha)/\alpha]$ for the reaction: $Z^= + H^+ \overset{K_1}{\rightleftharpoons} ZH^{\pm -}$								

[a] Titrations with NaOH and HCl are described by (−)ve and (+)ve values, respectively. [b] Data points used. [c] Parentheses include the standard deviations in the last digit. [d] R = correlation coefficient. [e] Log K_i = log K_i^o + $(n_i - 1)\log[(1-\alpha)/\alpha]$.

2.3.3. Copolymerization of hydrochloride salt 12 and maleic acid (2). For the experiment under entry 5, Table 1, a mixture of hydrochloride salt **12** (1.56 g, 5.0 mmol) and **2** (0.640 g, 5.5 mmol) in water (0.94 g; monomers/water wt ratio:70 : 30) was stirred at 98 °C in a RB flask attached to a condenser and maintained under a positive atmosphere of N_2. Then, initiator (APS) was added in two equal portions (2 × 200 mg) with an interval of 5 min. Exothermic polymerization ensued to give a viscous solution. After stirring at 98 °C for 15 min, the mixture was cooled and dialyzed against 0.1 M HCl for 24 h and subsequently against deionized water. The dialyzed mixture was treated with concentrated HCl (0.50 g, 37%, 5.0 mmol) and freeze-dried to obtain alternate cationic copolymer **14** as a white powder (1.29 g, 66%). Found: C 47.4; H 7.5; N 3.4%. $C_{17}H_{31}ClNO_7P$ requires C 47.72; H 7.30; N 3.27. δ_P (200 MHz, D_2O): 25.85 (m, minor, 5%, 1P), 31.16 (m, major, 95% 1P); ν_{max} (KBr): 3483 (broad), 3208, 3082, 2990, 2939, 2703, 1724, 1639 (very weak), 1612, 1452, 1399, 1201, 1027, 966, 801, 704 and 610 cm^{-1}.

2.3.4. Ester hydrolysis of polyampholyte 15 to polyzwitterion 4. A solution of polyampholyte **15** (obtained from entry 6, Table 1) (1.5 g, 3.83 mmol) in 6 M HCl (20 cm^3) was stirred at 90 °C under N_2 for 24 h. The solution of the resulting cationic polymer **3** upon depletion of HCl during dialysis (24 h)

Table 3 Protonation of polymer **4** ($ZH^{\pm}$) at 23 °C

Run	$ZH_2^{\pm}$ (mmol)	C_T[a] (mol dm^{-3})	α-Range	pH-range	Points[b]	Log K_1^{oc}	n_1[c]	R^{2d}
Polymer **4**								
1	0.2416 ($ZH_4^{\pm}$)	−0.09594	0.54–0.09	4.65–5.72	7	4.76	0.99	0.9842
2	0.2701 ($ZH_4^{\pm}$)	−0.09594	0.52–0.088	4.68–5.66	9	4.80	1.03	0.9902
3	0.2982 ($ZH_4^{\pm}$)	−0.09594	0.51–0.11	4.74–5.62	9	4.74	0.96	0.9965
Average						4.77 (3)	0.99 (4)	
Log $K_4^e = 4.77 - 0.01 \log[(1-\alpha)/\alpha]$ for the reaction: $ZH_3^{\pm -} + H^+ \overset{K_4}{\rightleftharpoons} ZH_4^{\pm}$								
1	0.2416 ($ZH_4^{\pm}$)	−0.09594	0.89–0.10	6.00–8.71	9	7.27	1.59	0.9845
2	0.2701 ($ZH_4^{\pm}$)	−0.09594	0.87–0.12	6.05–0.8.65	11	7.31	1.64	0.9907
3	0.2982 ($ZH_4^{\pm}$)	−0.09594	0.86–0.18	6.11–8.28	8	7.21	1.62	0.9827
Average						7.26 (3)	1.62 (3)	
Log $K_3^e = 7.26 + 0.62 \log[(1-\alpha)/\alpha]$ for the reaction: $ZH_2^{\pm =} + H^+ \overset{K_3}{\rightleftharpoons} ZH_3^{\pm -}$								
1	0.2416 ($ZH_4^{\pm}$)	−0.09594	0.87–0.37	9.17–10.43	10	10.15	1.22	0.9982
2	0.2701 ($ZH_4^{\pm}$)	−0.09594	0.85–0.35	9.18–10.42	12	10.20	1.29	0.9894
3	0.2982 ($ZH_4^{\pm}$)	−0.09594	0.81–0.30	9.19–10.45	9	9.93	1.31	0.9913
Average						10.09 (14)	1.27 (5)	
Log $K_2^e = 10.09 + 0.27 \log[(1-\alpha)/\alpha]$ for the reaction: $ZH^{\pm \equiv} + H^+ \overset{K_2}{\rightleftharpoons} ZH_2^{\pm =}$								

[a] Titrations with NaOH is described by (−)ve values. [b] Data points used. [c] Parentheses include the standard deviations in the last digit. [d] R = correlation coefficient. [e] Log K_i = log K_i^o + $(n_i - 1)\log[(1-\alpha)/\alpha]$.

against deionized water gave PZ **4**. Initially polymer **3** was soluble in the presence of HCl, however as the dialysis was continued PZ **4** started separating out within 1 h as a jelly material. The heterogeneous mixture was freeze-dried to obtain **4** (1.22 g, 95%). The polymer thus obtained is spectrally (IR, NMR) similar to **4** obtained *via* copolymerization of **1** and **2** (*vide supra*).

2.4. Potentiometric titrations

The basicity or protonation constants (K) of several basic centers in the synthesized polymers were determined in CO_2-free water using procedures reported elsewhere.[19,20] As described in Tables 2 and 3, a certain number of millimole of a repeating unit of PA **15** (ZH_2^{+-}) or PZ **4** ($ZH_2^{\pm}$) in water (200 cm^3) was titrated by stepwise addition of 0.05–0.15 mL of ≈0.1 M NaOH or HCl. Because of water-insolubility, PZ **4** ($ZH_2^{\pm}$) was first dissolved using 1–1.5 mL of 0.09594 M NaOH, then the titration was continued. Log K_is were calculated using the pH values and the Henderson–Hasselbalch equation (eqn (2); Scheme 3). While all three log K_is ($i = 2, 3, 4$) associated with the protonation of PDA (=) **17** were determined, two (log K_1 and log K_5) of the five log K_is associated with the protonation of basic centers in PTA (= =) **8** could not be determined. Log K_5, associated with the equilibrium: **4** ($ZH_4^{\pm}$) + H^+ ⇋ (ZH_5^+) **3**, was not determined since PZ (±) **4** was water-insoluble, while log K_1 involving ($Z^{=\ =}$) **8** + H^+ ⇋ **7** ($ZH^{\pm\ \equiv}$) would require a large amount of NaOH to generate a meaningful concentration of (:$Z^{=\ =}$) **8**.

2.5. Antiscalant behavior of the synthesized polymers

A solution containing Ca^{2+} (2598 mg L^{-1}) and SO_4^{2-} (6300 mg L^{-1}), which is supersaturated with respect to $CaSO_4$, was used to investigate scale formation at 40 ± 1 °C as described[21] using its supersaturated solution in the presence of antiscalants **4** (derived from hydrolysis of polymer **15** from entry 6, Table 1) and **15** (Table 1, entry 6). Stock solution of antiscalant **4** was prepared by dissolving it in the presence of minimum quantity of $NaHCO_3$. At a certain time, called induction time, the conductivity decreased suddenly as a result of scale formation (Table 4). Any turbidity is confirmed by visual inspections.

3. Results and discussion

3.1. Synthesis of alternate copolymers

The results of the alternate cyclopolymerization of diallyl amine salts **1**, trivalent amine **11** and amine salt **12** with maleic acid **2** are given in Table 1. Cationic monomer **1**/maleic acid **2** copolymerization afforded polycation (PC) (+) **3** which was changed to polyzwitterion (PZ) (±) **4** during dialysis as a result of depletion of HCl (Scheme 1). Changing 1 : 1 monomer stoichiometry (*i.e.* changing the feed ratio) did not change the composition of polymer **4** as indicated by its identical IR and NMR spectra (*vide supra*) as well as elemental analyses (entries 1–4, Table 1) which indicated the formation of alternate copolymers.

Similar homopolymerization of *N*-alkyldiallylammonium chloride as well as its copolymerization with maleic acid in aqueous solution using 5 mol% 2,2′-azobis[2-methyl-*N*-(2-hydroxyethyl)propionamide] (VA086) as initiator for 48 h at 75 °C have been reported to give polymers in low yields (typically below 20%).[22,23] High initiator concentrations (up to 5 mol%) were necessary to obtain the polymers, while the use of other initiators (ammonium persulfate, hydrogen peroxide) did not improve the yields.[22,23] It is interesting to note in the current work, the use of ammonium persulfate (≈10 mol%) at higher polymerization temperature (98 °C) for a short duration (20 min) afforded the alternate PZ **4** in very good isolated yields (≈70%) (entries 1–4, Table 1). Note that the monomer conversions were ≈90% as determined by ^{1}H NMR analyses; during dialysis, however, low MW molecules left the dialysis tube.

The reactivity ratios for diallylamines/maleic acid copolymerization are very much close to zero, thereby indicating a perfect alternating copolymerization.[23] Several reports suggested that the alternating incorporation of the amine and maleic acid monomers may be attributed to the formation of ions pairs (akin to **13**, Scheme 2) in solution and their polymerization.[24,25] In the current work, both the monomers **1** and **2** are fully protonated, and the extent of ionization in a highly concentrated solution (70 : 30 wt ratio of monomer/water) is rather low. This led us to believe that as in the case of the alternating copolymer of styrene and maleic anhydride, the copolymerization described here points towards a preferential combination of electron-rich **1** and electron-poor **2** monomers. Similar argument might as well be put forward against the formation of monomer ion-pair for the cyclopolymerization of **2**/**12** (Scheme 2). The stronger binding ability of Cl^- for the positive nitrogen would preclude the formation of ion-pair involving maleate anion $HO_2CCH{=}CHCO_2^-$.

The polymerization of **11**/**2** monomer-pair as depicted by structure **13** (entries 6–8, Table 1) as well as copolymerization of **12** and **2** (entry 5, Table 1) afforded the same polyampholyte (PA) **15** (Scheme 2). The copolymerization under entry 5 was even run in the presence of NaCl which has excellent ability to bind to positive nitrogen, thereby preventing the maleate to be a part of the ion-pair. The results thus indicate that ion-pair formation is not necessary to form alternate copolymers, rather it is the result of near zero reactivity ratios of the monomers. Note that while the initiator APS afforded copolymers in 20 min reaction-time in very good yields (entries 1–7), the azo initiator AMPH gave polymer **15** in lower yield even after carrying out the polymerization for a duration of 48 h at 80 °C (entry 8).

The isolated yields of the polymers as obtained after dialysis are given in Table 1. However, the actual percent conversion (written in parentheses, Table 1) was determined by ^{1}H NMR analyses (as described below) of the crude reaction mixture. The area **A** under δ 5.5–6 ppm accounts for 6 olefinic protons of unreacted monomer **12** or **13**, while its remaining 20H would appear in the range δ 1.2–4.1 ppm accounting for an area of **B** [*i.e.* (A/6) × 20] (Fig. 2a). The total integrated area C in the range δ 1.0–4.1 ppm would belong to area integration of 28H (26H from repeating unit of **12** and 2H from maleic acid **2**) of polyzwitterion **15** (Fig. 2c) and 20H of unreacted monomer **12**. The

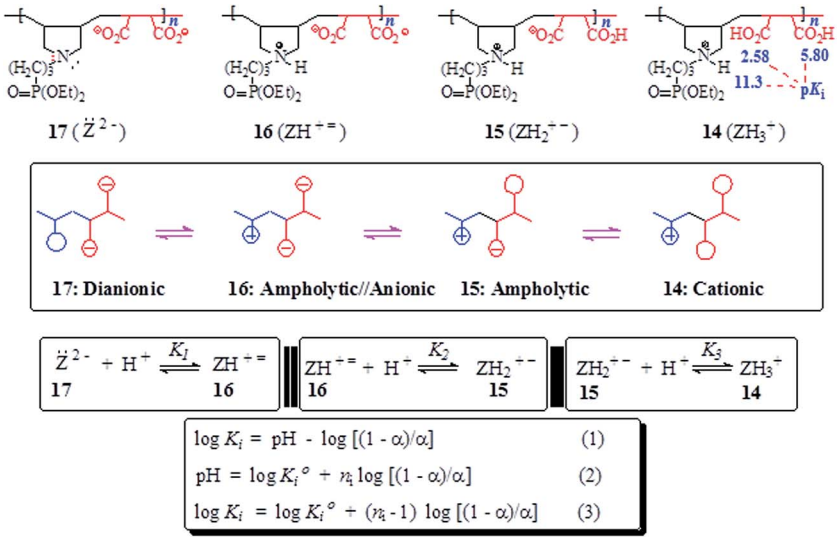

Scheme 3 pH induced changes in the charge types and densities in the backbone of **14–17**.

area D of the polymer alone would then equate to $(C - B)$. The percent conversion was then calculated using integration of 1H of the polymer **15** and monomer **12** as: $100 \times (D/28)/[(D/28) + A/6]$. In a similar fashion, the percent conversion to **4** was determined.

3.2. Solubility behavior

Unlike the majority of electroneutral polymers, PA (+ −) **15** was found to be water-soluble. A possible rationale could be that both the positive nitrogens as well as the negative charge centers on the carboxyl are in a crowded environment, thus preventing them from intragroup, intra- and inter-chain associations required for the manifestation of ampholytic interactions.[2] The relatively large separation between the charge centers and their difficulty in transiting to a curled conformation are expected to increase the dipole moment μ of the ampholytic motifs. Increased dipole moment would lead to increased hydrophilicity and solubilty.[26,27]

Polyzwitterion (±) **4**, however, was found to be water-insoluble. pK_1 of PO_3H_2 in (+) **3** and pK_1 of CO_2H in (+) **14** is expected to be <2 and ≈4, respectively (*vide infra*). As a result, PO_3H^- in (±) **4** has more dispersed charge than CO_2^- in (+ −) **15**, thereby making the former motifs less hydrated and hence more capable of manifesting zwitterionic interactions with the positive nitrogens.[28] Polyzwitterion **4** was insoluble in salt free water both at room and elevated temperatures (40–70 °C). At 4 wt% in 0.5 M NaCl, PZ **4** was soluble at 0 °C, but became cloudy while heating (50 °C). The lower critical solution temperature (LCST) was determined to be 27 °C. As expected, the PZ was found to be soluble in the presence of NaOH to generate polymers **5–8** (Scheme 1). In the presence of HCl (0.1 M), PZ **4** is transformed to cationic **3** which was found to be water-soluble.

3.3. TGA curves, FT-IR and NMR spectra

The PZ **4** was found to be more stable than PA **15** according to their TGA curves (Fig. 1). For PZ **4**, a 6% weight loss up to 200 °C was accounted for the removal of moisture. An additional 7% loss in the range 200–270 °C resulted from the elimination of water as a result of formation of cyclic anhydrides from two neighboring CO_2H groups. A loss of ≈23% in 275–400 °C range is attributed to the release of maleic anhydride units from the polymer backbone.[22,29] The total loss up to 400 °C was found to

Table 4 Percent scale inhibition in the presence of PZ **4** and PA **15** in 3 CB[b] supersaturated $CaSO_4$ solution at 40 °C

Entry	Sample (ppm)	Percent inhibition at times (min) of						Induction time (min)
		30	60	120	1000	2000	14 000	
Polymer **4**								
1	5	100	100	99	—	—	—	170
2	10	100	100	100	100	100	—	2100
3	15	100	100	100	100	100	100	—[a]
4	20	100	100	100	100	100	100	—[a]
Polymer **15**								
5	20	19	5	—	—	—	—	10

[a] No induction time was observed. [b] Three times the concentration of Ca^{2+} and SO_4^{2-} found in the concentrated brine of an RO plant.

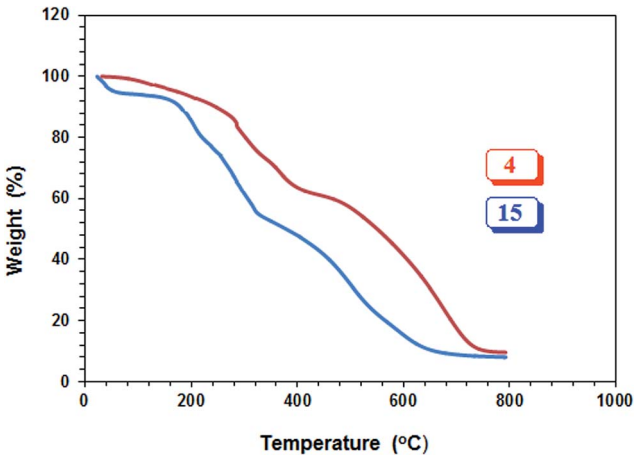

Fig. 1 TGA curves of **4** and **15**.

be 36%, while the maleic acid units accounts for 34.6% thus giving credence to the described losses mentioned above. A further loss of 36% in the 400–800 °C range is linked to the detachment of phosphonate pendants.

The IR spectra of (±) **4**, (+) **14** and (+ −) **15** revealed a strong absorption band at ≈1720 cm^{-1} attributed to C=O stretch of CO_2H group. While the absorption peak for CO_2^- ions in **15** appeared at 1575 cm^{-1},[30] the corresponding peak was absent in the spectrum of **14**. Fig. 2 and 3 display the NMR spectra of several polymers. The absence of any signal for residual alkene protons at δ 5.5–6 ppm or carbons at ≈δ 125 ppm suggested the degradative chain transfer[31] by abstraction of allylic hydrogens or coupling process for the termination reaction. As compared to homopolymer **18**[14] (Scheme 2) (Fig. 2b), the spectrum of copolymer (+ −) **15** (Fig. 2c) is broadened presumably as a result of its compact coil conformation and hydrophobic association in aqueous solution.[22] The presence of a peak near 180 ppm proves the incorporation of maleic acid in the copolymer (Fig. 3c–e). Note that the ^{13}C NMR signals attributed to the carbons in the polymer backbone marked 'a' and 'b' are missing in the spectrum of (+ −) **15** (Fig. 3e), while the carbons away from the polymer backbone give well resolved signals. This behavior is a characteristic of many polymerized surfactant, pointing to an immobilization of the polymer backbone. Note that the ester carbons marked 'h' and 'g' (Fig. 3a, d and e) are

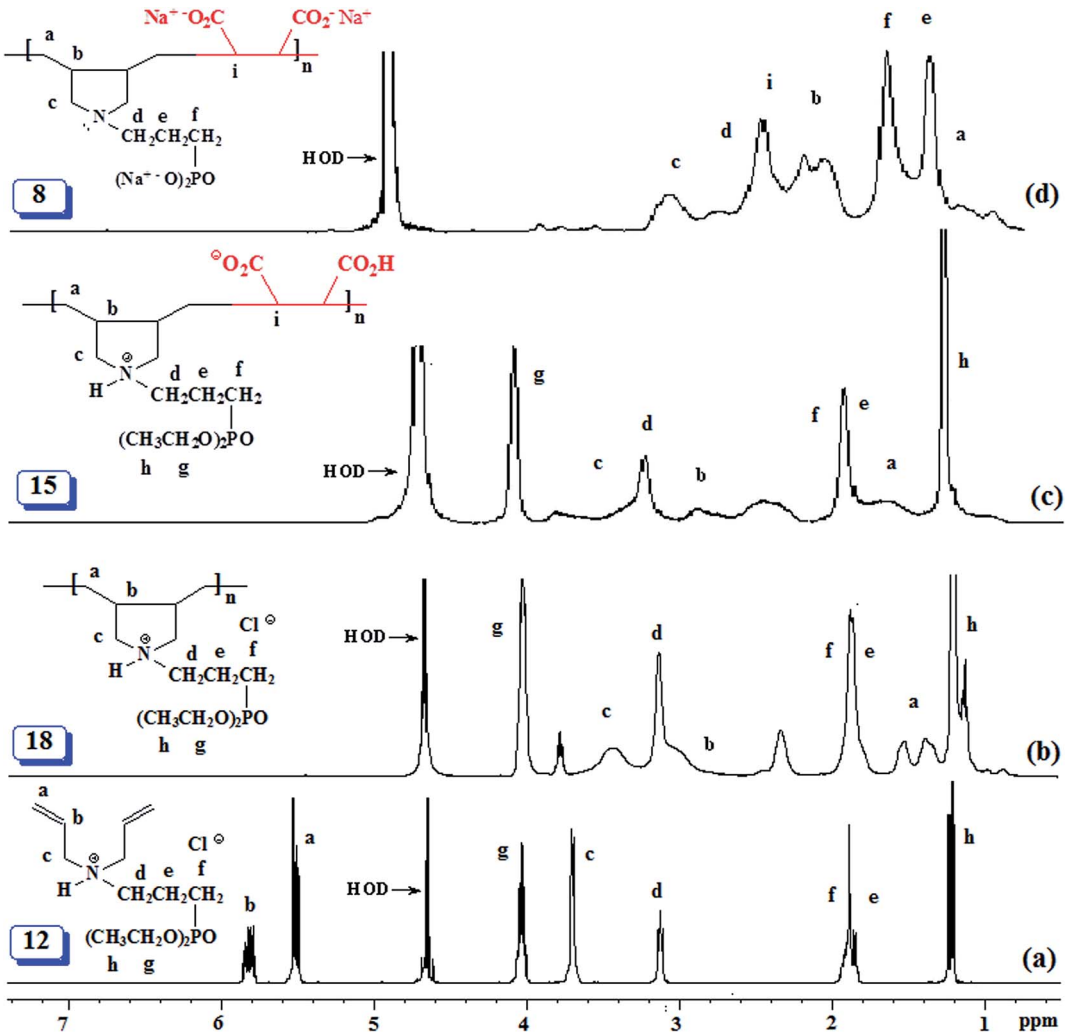

Fig. 2 ^1H NMR spectrum of (a) **12**, (b) **18**, (c) **15**, and (d) **8** in D_2O.

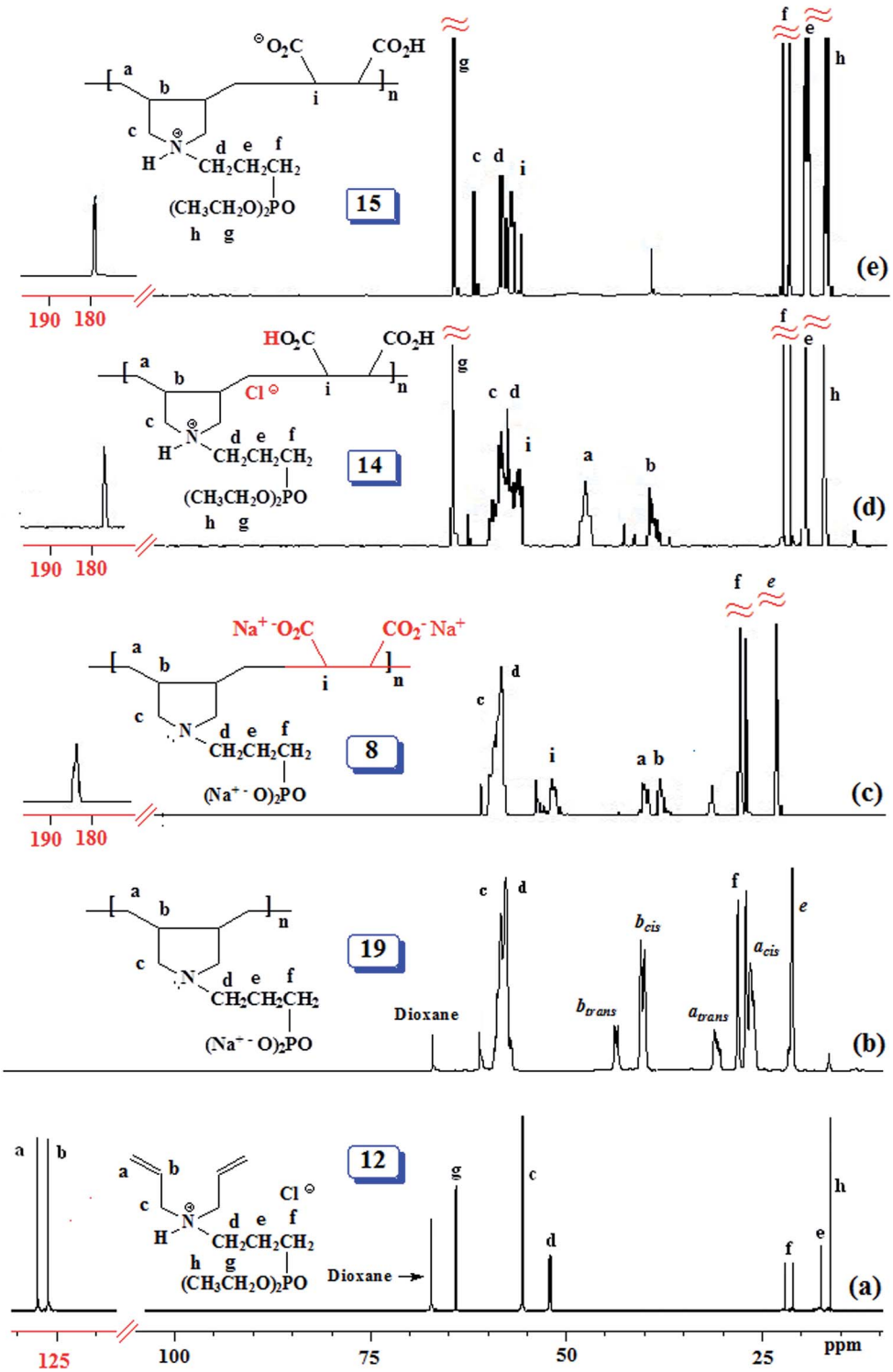

Fig. 3 ^{13}C NMR spectrum of (a) **12**, (b) **19**, (c) **8**, (d) **14**, and (e) **15** in D_2O.

absent in the NMR spectra of the hydrolyzed polymers (Fig. 3b and c).

The ^{13}C NMR spectra shed some light on the monomer sequence of repeating units in the current polymers. The backbone carbon marked 'a' for homopolymer **19** around δ 27 ppm (Fig. 3b) is shifted downfield in the copolymers' spectra (Fig. 3c and d); the absence of any residual signal around δ 27 ppm points toward a perfect alternation of the repeating units.

3.4. Viscosity measurements

The viscosity values of PA (+ −) **15** (entry 6, Table 1) are presented in Fig. 4. The antipolyelectrolytic[32] behavior of the

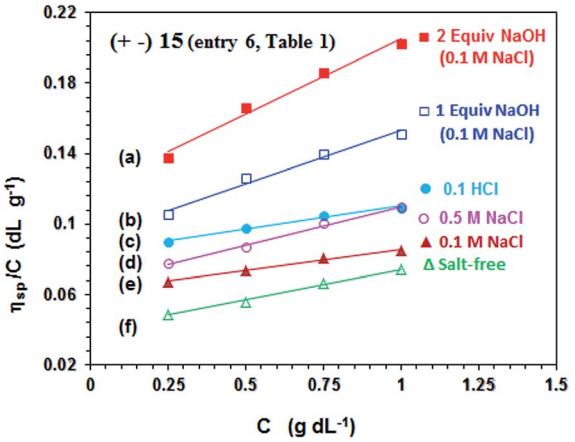

Fig. 4 The viscosity behavior at 30 °C of polyampholyte **15** (entry 6, Table 1) (a) ■ in the presence of 2 equiv. NaOH in 0.1 M NaCl, (b) □ in the presence of 1 equiv. NaOH in 0.1 M NaCl, (c) ● in 0.1 M HCl, (d) ○ in 0.5 M NaCl, (e) ▲ in 0.1 M NaCl, and (f) Δ in salt-free water.

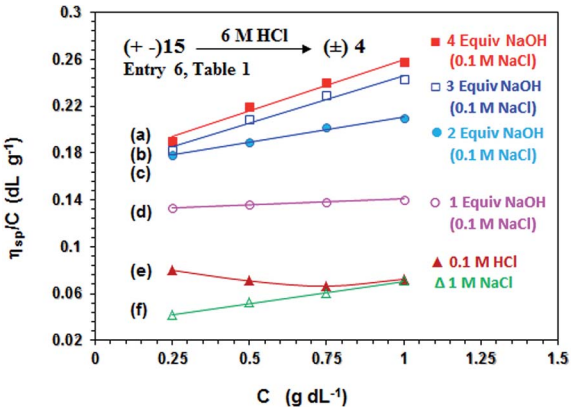

Fig. 5 The viscosity behavior at 30 °C of polyzwitterion **4** (prepared by acid hydrolysis of **15** from entry 6, Table 1) (a) ■ in the presence of 4 equiv. NaOH in 0.1 M NaCl, (b) □ in the presence of 3 equiv. NaOH in 0.1 M NaCl, (c) ● in the presence of 2 equiv. NaOH in 0.1 M NaCl, (d) ○ in the presence of 1 equiv. NaOH in 0.1 M NaCl, (e) ▲ in 0.1 M HCl, and (f) Δ in 1.0 M NaCl.

polyampholyte is demonstrated as evinced by the direct proportionality of the viscosity with the NaCl concentrations (*cf.* Fig. 4d–f). The ampholytic dipole may not be electroneutral; a residual negative charge on the dipole is a consequence of greater neutralization of N^+ by Cl^- as compared to the binding ability of CO_2^- by Na^+.[33–35] The magnitude of excess negative charge on a dipole increases with increasing salt concentrations, thereby leading to increasing repulsion among the dipole centers and increasing viscosity.

The pH-induced changes in the polymer backbone of **14–17** are illustrated in Scheme 3. In 0.1 M HCl, PA (+ −) **15** becomes CPE (+) **14**; increased hydrodynamic volume as a result of repulsion among positive charges leads to the increase in the viscosity (Fig. 4c). PA (+ −) **15** is transformed to polyampholyte/anion (+ =) **16** and polydianion (=) **17** upon treatment with one and two equivalents of NaOH, respectively. As expected, the viscosity increases in the presence of NaOH (Fig. 4a and b), the larger charge imbalance in (=) **17** makes it more viscous.

In order to correlate the viscosity values of polyphosphonate ester and polyphosphonic acid, PA (+ −) **15** (entry 6, Table 1) is converted to PZ (±) **4** having identical degree of polymerization. Viscosity plots for PZ (±) **4** are shown in Fig. 5. The pH-induced changes in the polymer backbone of **4–8** are illustrated in Schemes 1 and 4. In the presence of one, two, three and four equivalents of NaOH (per repeating unit), PZ (±) **4** is expected to generate polyzwitterion/anion (PZA) (± −) **5**, polyzwitterion/dianion (PZDA) (± =) **6**, polyzwitterion/trianion (PZTA) (± ≡) **7**, polytetraanion (PTA) (= =) **8**, respectively, as the dominant species involved in mobile equilibria with other species. With the increase in NaOH concentrations, the imbalance in favor of negative charges increases, thereby forcing the polymer backbone to adapt more extended conformation to minimize repulsion. This would result in the increase of viscosity values in the order: (= =) **8** > (± ≡) **7** > (± =) **6** > (± −) **5** as determined experimentally (*cf.* Fig. 5a–d). PZ (±) **4** is insoluble in salt-free water; however, its viscosity plot in 1.0 M NaCl is shown in Fig. 5f. The viscosity plot for PZ (±) **4** in 0.1 M HCl is found to be concave upward, presumably as a result of increasing dissociation to (PZA) (± −) **5** with dilution (Fig. 5e).

The increase in charge imbalance in a polymer backbone leads to an increase in excluded volume, which has been used to rationalize the solution properties of ionic polymers.[36–39] Polyzwitterion/anion (PZA) (± −) **5** and polyampholyte/anion (+ =) **16**, having identical degree of polymerization, were generated by treating (±) **4** and (+ −) **15**, respectively, with one equivalent NaOH. Ionic polymers (± −) **5** and (+ =) **16** having similar imbalances in favor of negative charges were found to have intrinsic viscosity $[\eta]$ of 0.131 dL g^{-1} (Fig. 5d) and 0.0928 dL g^{-1} in 0.1 M NaCl (Fig. 4b). Likewise, polyphosphonic acid derivative polyzwitterion/dianion (PZDA) (± =) **6** was determined to have higher $[\eta]$ value of 0.168 dL g^{-1} (Fig. 5c) than the $[\eta]$ value of 0.120 dL g^{-1} of diester derivative polydianion (=) **17** having identical DP and charge imbalances (Fig. 4a). The lower $[\eta]$ values for the ester polymers **16**/**17** could be attributed to the greater hydrophobic character owing to the presence of ethyl groups in the pendants.

As reported earlier[22] and found in the current work, the molar masses of the polymers could not be obtained by GPC presumably owing to the strong interaction of the materials in the GPC column with the amine and carboxy motifs of the polymers. The lower intrinsic values, however, suggest lower molar masses of the polymers because of using higher doses of initiator and a higher temperature of ≈100 °C. Moreover, the degradative chain transfer involving abstraction of allylic hydrogen in the diallylamine salts also lowers the molar masses.[31]

The molecular weights of the polyzwitterion (±) **4** was estimated from the viscosity data by Mark–Houwink equation ($[\eta] = KM_v^a$),[40] using $K = 1.12 \times 10^{-4}$ dL g^{-1} and $a = 0.82$, which are given for poly(diallyldimethylammonium chloride) for a temperature of 25 °C in 1 M NaCl.[41] The $[\eta]$ of (±) **4** was determined to be 0.0324 dL g^{-1} (Fig. 5f) which translates into a viscosity average molecular weight $M_v \approx 16\,640$ g mol^{-1}

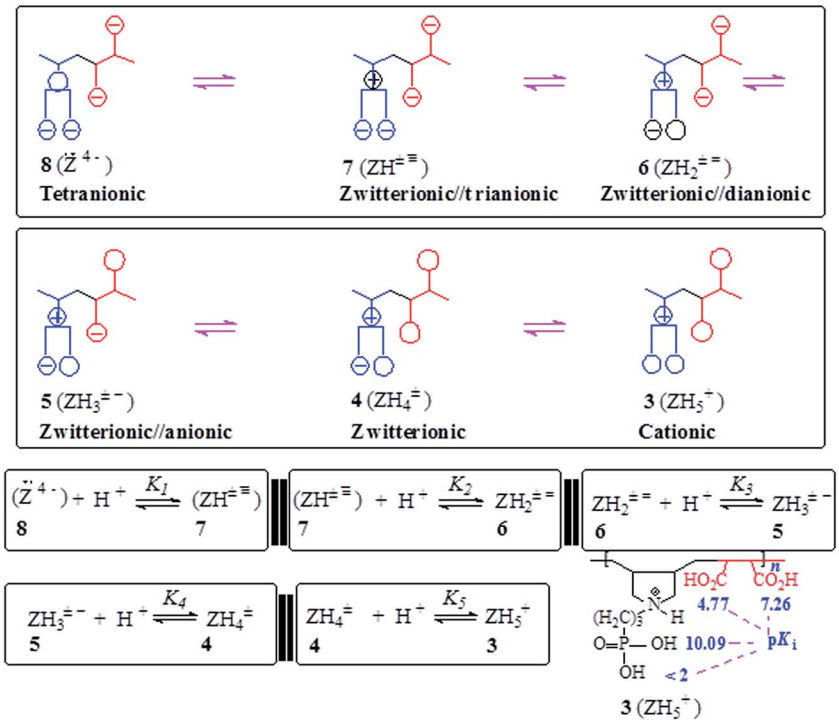

Scheme 4 pH induced changes in the charge types and densities in the backbone of **3–8**.

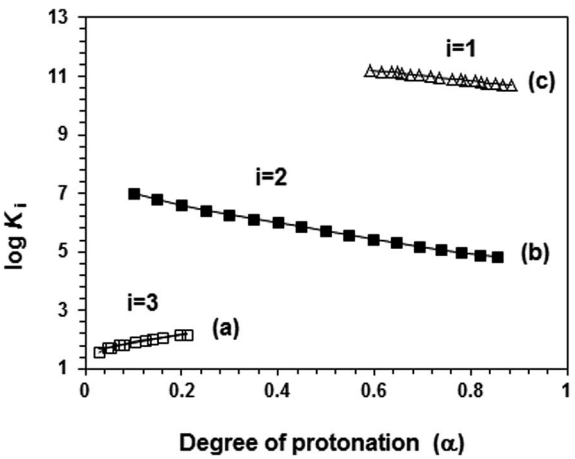

Fig. 6 Plot for the apparent log K_i *versus* degree of protonation (α) in salt-free water (a) □ (log K_3, run 1, Table 3), (b) ■ (log K_2, run 3, Table 3) and (c) Δ (log K_3, run 3, Table 3).

corresponding to a degree of polymerization of approximately 99 (*i.e.* number of structural units).

3.5. Basicity constant

The apparent basicity constant (K) of several functional centers in polymer (=) **17** and (= =) **8** is described by eqn (3) (Scheme 3) where log K^o = pH at $\alpha = 0.5$ and $n = 1$ observed for basicity constant of small molecules. The slope and intercept of the straight-line plot of pH *vs.* log$[(1-\alpha)/\alpha]$ gave the values of 'n' and log K^o, respectively. In salt-free water, basicity constant log K_1^o, log K_2^o and log K_3^o were determined to be 11.3, 5.80 and 2.58, respectively, with the corresponding n_1, n_2 and n_3 values of 1.71, 2.38 and 0.41 (Table 2).

The n values >1 or <1 reflects the "apparent" nature of the basicity constant since the basicity constant changes with the degree of protonation.[42,43] A measure of the polyelectrolyte index n is shown in Fig. 6 displaying variation of K with α signifying a polyelectrolyte effect. With increasing α, a gradual decrease of log K_1^o [involving ($Z^{=}$) **17** + H^+ ⇋ ($ZH^{+\ =}$) **16**] and log K_2^o [involving ($ZH^{+\ =}$) **16** + H^+ ⇋ ($ZH_2^{+\ -}$) **15**] is a result of decreasing overall negative charges that induces protonation. The n values > or <1 confirm the consequence of entropy effects.[42,44] PDA (=) **17** having greater charge imbalance is more hydrated than (+ =) **16** which in turn is more hydrated than (+ −) **15**. With each protonation, water molecules are released from the hydration shell of the repeating unit that is being protonated. With increasing α, the excess average negative charge in the polymer backbone decreases as does the average number of water molecules in the hydration shell of a repeating unit. Therefore, there will be release of lesser and lesser number of water molecules from the polymer backbones with increasing α, and the associated entropy change dictates the decrease of K with increasing α. The exothermic ΔH^o has been reported to be independent of α, the ΔG^o is thus controlled by the entropy term.[44]

The n_3 value associated with log K_3^o [involving ($ZH_2^{+\ -}$) **15** + H^+ ⇋ (ZH_3^+) **14**] was found to be 0.41. The n value <1 is characteristic of a compact conformation arising out of the presence of ampholytic and zwitterionic motifs. The approach of protons towards ($ZH_2^{+\ -}$) **15** becomes easier with the increasing degree

of protonation.[45,46] The protonation constant log K_3 increases progressively with increasing α (Fig. 6a). The macromolecular coil expands as a result of a decrease in the density of the ampholyte motifs (*cf.* viscosity curves Fig. 4c *versus* Fig. 4e), thereby exposing the polymer backbone for easier access to protonation. With each protonation, the imbalance in favor of positive charges on the backbone increases. Increased hydration, as a result, leads to entropically favorable release of a greater number of hydrated molecules during protonation.

For polytetraionic (= =) **8**, log K_2^o, log K_3^o and log K_4^o were determined to be 10.09, 7.26 and 4.77, respectively with the corresponding n values of 1.27, 1.62 and 0.99. Note that the pK_a of an acid (HA) is the log K_b (*i.e.* log[basicity constant]) of its conjugate base (A^-). For the pentaprotic acid (ZH_5^+) **3** and triprotic acid (ZH_3^+) **14**, the pK_is of several protic centers are shown in Schemes 3 and 4. The values of pK_1 and pK_5 were not determined for the reasons mentioned in the experimental, however the pK_1 of (ZH_5^+) **3** (Schemes 1 and 4) is estimated to have a value of <2 since methanephosphonic acid itself is known to have pK_1 value of 2.12. The considerable difference is observed in the acidity of the first carboxylic acid groups in **14** (with pK value 2.58) [involving (ZH_3^+) **14** $\leftrightharpoons$ (ZH_2^{+-}) **15** + H^+] (Scheme 3) and **4** (with pK value of 4.77) [involving ($ZH_4^{\pm}$) **4** $\leftrightharpoons$ ($ZH_3^{\pm -}$) **5** + H^+] (Scheme 4). While the higher acidity of the first CO_2H in (ZH_3^+) **14** is attributable to the electrostatic attraction[30,47,48] associated with polyampholyte motifs (ZH_2^{+-}) in its conjugate base **15**, the difficulty associated with the removal of a proton from ($ZH_4^{\pm}$) **4** involves the transformation of a zwitterionic motif to an energetically less favorable zwitterion/anion ($ZH_3^{\pm -}$) **16** ampholytic/anion ($ZH^{+ =}$).

3.6. Scale inhibition study

The inlet feed water in a reverse osmosis (RO) process produces product water and rejects brine. The supersaturation of any of the dissolved salts in the reject brine stream leads to its precipitation. The percent scaling inhibition (PSI) is calculated using eqn (4):

$$\mathrm{PSI} = \frac{[Ca^{2+}]_{\text{inhibited }(t)} - [Ca^{2+}]_{\text{blank }(t)}}{[Ca^{2+}]_{\text{inhibited }(t_0)} - [Ca^{2+}]_{\text{blank }(t)}} \times 100 \qquad (4)$$

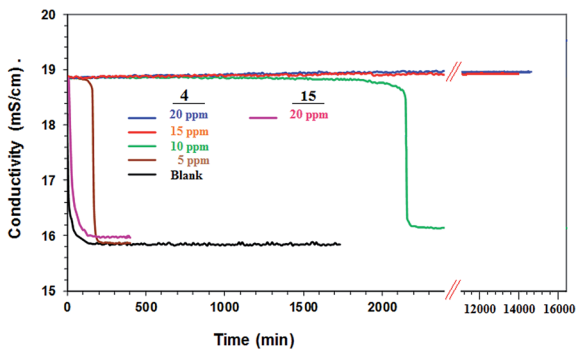

Fig. 7 Conductivity of a supersaturated solution of $CaSO_4$ in the presence (5, 10, 15, 20 ppm) of **4** and **15** (20 ppm) and in the absence (blank) of antiscalant.

where [Ca^{2+}] describes concentration at time zero and t, in the presence (inhibited) and absence (blank) of antiscalant.

The scaling behavior of a supersaturated solution of $CaSO_4$ containing Ca^{2+} (2598 ppm) and SO_4^{2-} (6300 ppm) in the presence of synthesized polymers **4** and **15** was investigated. These are three times the concentration of Ca^{2+} and SO_4^{2-} found in the reject brine denoted as 1 CB (*i.e.* concentrated brine) from a RO plant.[49] The PSI by **4** and **15** at various concentrations of the antiscalants is given in Table 4. The onset of $CaSO_4$ precipitation is marked by a sudden drop in the conductivity (Fig. 7). To our satisfaction, the presence of a small concentration (5 ppm) of **4** registered a 99% scale inhibition for about 120 min. In the presence of 10, 15 and 20 ppm of the antiscalant, it registered a PSI of ≈100% for 2000 min. It is indeed astonishing to observe that the antiscalant **4**, at a concentration of 15 or 20 ppm, PSI remains ≈100% even after 14 000 min (*i.e.* 9.7 days). An antiscalant needs to be effective at least for a minimum period of ≈30 min which is the residence time for the brine in the osmosis chamber. Note that PA **15** containing ester motifs was ineffective as an antiscalant (Fig. 7) (Table 4); the precipitation of $CaSO_4$ occurred within 10 min as confirmed by a large drop in conductivity. The current PZ **4** has even much superior antiscalant efficacy than its corresponding homopolymer **9** or **10** (Scheme 1).[14] As shown in Fig. 7, the onset of precipitation occurs after an induction period. A sharp drop in conductivity is attributed to an accelerated growth of $CaSO_4$ crystals. At a concentration of 5 and 10 ppm, the induction time was observed to be 170 and 2100 min, respectively. For a duration of 14 000 min, induction time was not observed in the presence PZ **4** (15 and 20 ppm). The antiscalant inhibits the crystal growth by complex formation with metal cations, thereby altering the crystal morphology at the time of nucleation.[50,51] The precipitation of gypsum, *i.e.* $CaSO_4$ in mineral form, is an undesirable occurrence in several processes like sea water desalination, water distillation, industrial water recovery and hydrometallurgical operations.[52] PZ **4** is remarkably efficient in prolonging the induction period, and thus has the potential to mitigate the membrane fouling as a result of scale formation.

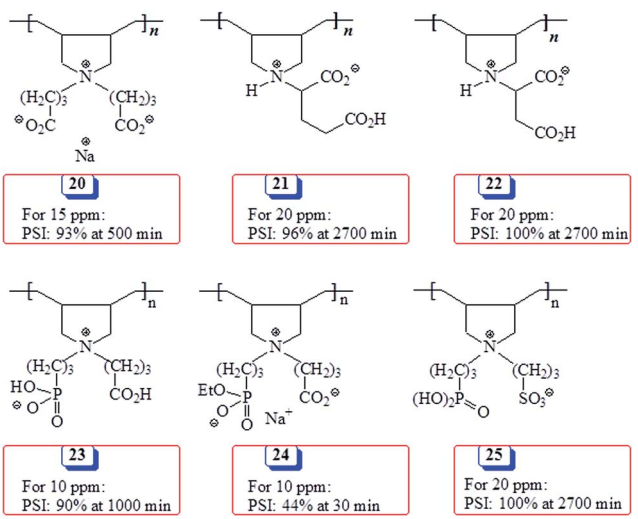

Scheme 5 Percent scale inhibition (PSI) of some antiscalants synthesized *via* cyclopolymerization protocol in literature.

In comparing the antiscalant activity of **4**, **15**, **9** or **10**, note that polymer **15** with ester motifs cannot bear negative charges on the phosphonate pendants and as such cannot effectively interfere with the positive Ca^{2+} during nucleation.[13–15] The repeating unit in **4** has a greater negative charge density than its homopolymer **9** or **10**. The greater negative charges in **4** not only disturb the nucleation process by adsorption onto the developing crystal, they also prevent the agglomeration (*i.e.* scale formation) by repulsion among the distorted crystals bearing excessive negative charges. The above rationale clearly accounts for the remarkable antiscalant activity of PZ **4**.

Some polyzwitterions (PZs) synthesized *via* cyclopolymerization and their effectiveness as antiscalants in terms of percent scale inhibition (PSI) under conditions like the current work are presented in Scheme 5. Note that PZ **23** performed much better than its counterpart **24** having a monoethyl ester group, thereby confirming the necessity of the presence of the completely hydrolyzed phosphonate motifs to be a better antiscalnt.[53] Glutamic acid-based PZ **21**,[54] aspartic acid-based PZ **22**[55] and PZ **25**[12] containing phosphonate and sulfonate pendants as well as **20**[56] containing carboxyl group in both pendants performed very well imparting similar PSIs. However, the current PZ **4** with greater negative charge density outperformed all the other PZs presented in Scheme 5.

4. Conclusions

Maleic acid has been copolymerized with diallylammionium monomers **1** and **12** using Butler's cyclopolymerization protocol to give alternate copolymers PZ **4** and CPE **14** having three-carbon spacer separating the phosphonate and amine motifs. Likewise, ion-pair generated by treating *N*,*N*-diallyl-3-(diethylphosphonato)propylamine **11** with maleic acid underwent copolymerization to give alternate PA **15**. To correlate the solution properties of **4** and **15**, diester groups in **15** were hydrolysed by 6 M HCl to generate **4**. The pH-induced changes of backbone charges in pH-responsive tetraprotic **4** and diprotic **15** having identical degree of polymerization were investigated in detail by viscometric technique. Several protonation constants of the $CO_2^-PO_3^{2-}$ and trivalent nitrogen in **8** and **17** have been determined by potentiometric titrations.

Evaluation of the antiscalant properties using supersaturated solution of $CaSO_4$ revealed that PZ **4** is remarkably effective in inhibiting the formation of calcium sulfate scale for days at 40 °C. The superiority of phosphonic acid motifs in **4** over the phosphonate ester motifs in **15** in scale inhibition is demonstrated as the latter is found to impart no scale inhibition.

Acknowledgements

The facilities provided by KFUPM are gratefully acknowledged.

References

1 G. B. Butler, *Cyclopolymerization and cyclocopolymerization*, Marcel Dekker, New York, 1992.
2 G. B. Butler, *J. Polym. Sci., Part A: Polym. Chem.*, 2000, **38**, 3451–3461.
3 S. Kudaibergenov, W. Jaeger and A. Laschewsky, *Adv. Polym. Sci.*, 2006, **201**, 157–224.
4 A. Laschewsky, *Polymers*, 2014, **6**, 1544–1601.
5 P. K. Singh, V. K. Singh and M. Singh, *e-Polym.*, 2007, **30**, 1–34.
6 F. C. McGrew, *J. Chem. Educ.*, 1958, **35**, 178–186.
7 O. C. S. Al-Hamouz and S. A. Ali, *J. Polym. Sci., Part A: Polym. Chem.*, 2012, **50**, 3580–3591.
8 Z. A. Jamiu and S. A. Ali, *RSC Adv.*, 2016, **6**, 31019–31030.
9 A. V. Dobrynin, R. H. Colby and M. Rubinstein, *J. Polym. Sci., Part B: Polym. Phys.*, 2004, **42**, 3513–3538.
10 A. Rabiee, A. Ershad-Langroudi and H. Jamshidi, *Rev. Chem. Eng.*, 2014, **30**, 501–506.
11 R. Kumar and G. H. Fredrickson, *J. Chem. Phys.*, 2009, **131**, 104901.
12 S. A. Haladu and S. A. Ali, *J. Polym. Sci., Part A: Polym. Chem.*, 2013, **51**, 5130–5142.
13 M. Turek, K. Mitko, K. Piotrowski, P. Dydo, E. Laskowska and A. Jakóbik-Kolon, *Desalination*, 2017, **401**, 180–189.
14 H. Shemer, D. Hasson and R. Semiat, Review of the state of the art of antiscalant selection, in *Mineral Scales in Biological and Industrial Systems*, ed. Z. Amjad, CRC Press, 2014, pp. 227–255.
15 M. Chaussemier, E. Pourmohtasham, D. Gelus, N. Pecoul, H. Perrot, J. Ledion, H. Cheap-Charpentier and O. Horner, *Desalination*, 2015, **356**, 47–55.
16 S. A. Ali, N. Y. Abu-Thabit and H. A. Al-Muallem, *J. Polym. Sci., Part A: Polym. Chem.*, 2010, **48**, 5693–5703.
17 I. W. Kazi, F. Rahman and S. A. Ali, *Polym. Eng. Sci.*, 2014, **54**, 166–174.
18 S. A. Ali, I. W. Kazi and N. Ullah, *Ind. Eng. Chem. Res.*, 2015, **54**, 9689–9698.
19 S. A. Ali, S. A. Haladu and H. A. Al-Muallem, *J. Appl. Polym. Sci.*, 2014, **131**, 40615.
20 S. A. Ali, N. Y. Abu-Thabit and H. A. Al-Muallem, *J. Polym. Sci., Part A: Polym. Chem.*, 2010, **48**, 5693–5703.
21 S. A. Haladu and S. A. Ali, *J. Polym. Sci., Part A: Polym. Chem.*, 2013, **51**, 5130–5142.
22 F. Rullens, M. Devillers and A. Laschewsky, *Macromol. Chem. Phys.*, 2004, **205**, 1155–1166.
23 J. E. Boothe, H. G. Flock and M. F. Hoover, *J. Macromol. Sci., Chem.*, 1970, **A4**, 1419.
24 J. C. Salamone, A. C. Watterson, T. D. Hsu, C. C. Tsai, M. U. Mahmud, A. W. Wisniewski and S. C. Israel, *J. Polym. Sci., Part C: Polym. Symp.*, 1978, **64**, 229.
25 J. C. Salamone, M. K. Raheja, Q. Anwaruddin and A. C. Watterson, *J. Polym. Sci., Part C: Polym. Lett.*, 1985, **23**, 655.
26 M. Galin, A. Chapoton and J.-C. Galin, *J. Chem. Soc., Perkin Trans. 2*, 1993, 545.
27 A. W. Lloyd, C. J. Olliff and K. L. Rutt, *Int. J. Pharm.*, 1996, **131**, 257.
28 D. J. Walsh and G. L. Cheng, *Polymer*, 1984, **25**, 499.
29 M. Hahn, W. Jaeger, R. Schmolke and J. Behnisch, *Acta Polym.*, 1990, **41**, 107.

30 Z. E. Ibraeva, M. Hahn, W. Jaeger, L. A. Bimendina and S. E. Kudaibergenov, *Macromol. Chem. Phys.*, 2004, **205**, 2464–2472.
31 G. B. Butler and R. J. Angelo, *J. Am. Chem. Soc.*, 1957, **79**, 3128–3131.
32 K. Nishida, K. Kaji, T. Kanaya and N. Fanjat, *Polymer*, 2002, **43**, 1295–1300.
33 M. Gao, K. Gawel and B. T. Stokke, *Eur. Polym. J.*, 2014, **53**, 65–74.
34 Z. Cao and G. Zhang, *Phys. Chem. Chem. Phys.*, 2015, **17**, 27045–27051.
35 S. Morozova, G. Hu, T. Emrick and M. Muthukumar, *ACS Macro Lett.*, 2016, **5**, 118–122.
36 P. G. Higgs and J. F. Joanny, *J. Chem. Phys.*, 1991, **94**, 1543–1554.
37 F. Candau and J. F. Joanny, *Polyampholytes (Properties in Aqueous Solution)*, ed. J. C. Salamone, CRC Press, Boca Raton, FL 7, 1996, pp. 5462–5476.
38 J. Wittmer, A. Johner and J. F. Joanny, *Europhys. Lett.*, 1993, **24**, 263–268.
39 R. Everaers, A. Johner and J. F. Joanny, *Europhys. Lett.*, 1997, **37**, 275–280.
40 H. Dautzenberg, W. Jaeger, J. Kötz, B. Philipp, C. Seidel, and D. Stscherbina, *Polyelectrolytes: Formation, Characterization and Application*, Carl Hanser Verlag, Munich, 1994, p. 218.
41 H. Dautzenberg, W. Jaeger, J. Kötz, B. Philipp, C. Seidel and D. Stscherbina, *Polyelectrolytes: Formation, Characterization and Application*, Carl Hanser Verlag, Munich, 1994, p. 223.
42 R. Barbucci, M. Casolaro, N. Danzo, V. Barone, P. Ferruti and A. Angeloni, *Macromolecules*, 1983, **16**, 456–462.
43 M. S. Bodnarchuk, K. E. B. Doncom, D. B. Wright, D. M. Heyes, D. Dini and R. K. O'Reilly, *RSC Adv.*, 2017, **7**, 20007–20014.
44 R. Barbucci, M. Casolaro, P. Ferruti and M. Nocentini, *Macromolecules*, 1986, **19**, 1856–1861.
45 R. Barbucci, M. Casolaro, M. Nocentini, S. Correzzi, P. Ferruti and V. Barone, *Macromolecules*, 1986, **19**, 37–42.
46 A. Fini, M. Casolaro, M. Nocentini, R. Barbucci and M. Laus, *Makromol. Chem.*, 1987, **188**, 1959–1971.
47 Y. Merle, *J. Phys. Chem.*, 1987, **91**, 3092–3098.
48 S. Mafe, V. Garcia-Morales and P. Ramirez, *Chem. Phys.*, 2004, **296**, 29–35.
49 F. H. Butt, F. Rahman and U. Baduruthamal, *Desalination*, 1995, **103**, 189–198.
50 H. David, S. Hilla and S. Alexander, *Ind. Eng. Chem. Res.*, 2011, **50**, 7601–7607.
51 R. J. Davey, *The Role of Additives in Precipitation Processes, Industrial Crystallization, Proc. Symp.*, ed. S. J. Jancic and E. J. de Jong, North-Holland Publishing Co., 8th edn, 1982, pp. 123–135.
52 G. Mazziotti di Celso and M. Prisciandaro, *Desalin. Water Treat.*, 2013, **51**, 1615–1622.
53 S. A. Ali, S. A. Haladu and A. M. Z. El-Sharif, *J. Polym. Res.*, 2016, **23**, 167–176.
54 Z. A. Jamiu, H. A. Al-Muallem and S. A. Ali, *Des. Monomers Polym.*, 2016, **19**, 128–137.
55 Z. A. Jamiu, H. A. Al-Muallem and S. A. Ali, *React. Funct. Polym.*, 2015, **93**, 120–129.
56 S. A. Ali, S. A. Haladu and A. M. Z. El-Sharif, *Macromol. Res.*, 2016, **24**, 163–169.